

The Role of Material Properties and Operating Conditions in Fatigue Life Prediction: An Experimental and Statistical Approach

Abdelhakim Djalab^{1*}

¹ Mechanical Engineering Department, Faculty of Technology, University of M'sila, Road of Bourdj Bou Arreiridj, M'sila 28000, Algeria

* Corresponding author, e-mail: abdelhakim.djalab@univ-msila.dz

Received: 12/1/2025 Accepted: 14/03/2025 Published: 28/04/2025

Abstract

Material fatigue is now an essential aspect of modern industrial engineering as it has a significant impact on the strength and reliability of mechanical components in industrial systems. The study of fatigue mechanisms under different operating conditions is critical to achieving durable, long-lasting designs.

This experimental study investigates the fatigue behaviour of locally fabricated materials subjected to rotational bending. The main objectives are to determine the fatigue limit for a given cycle and the endurance limit. In order to characterise the fatigue strength of the material, a group of identical specimens were subjected to cycles of a specific shape. To analyse the effect of three operational variables - hardness (H), surface roughness (Ra) and applied stress (σ) - on the life (number of cycles) of the specimens, experiments were carried out using a Taguchi L18 mixed design. In conclusion, the results were statistically analyzed using Response Surface Methodology (RSM) and Analysis of Variance. The findings show that the applied stress is the most significant factor affecting specimen fatigue (lifetime), contributing 38.53%, followed by hardness. Additionally, the high value of the coefficient of determination, derived from the Taguchi method and the developed RSM, clearly demonstrates a strong correlation between the predicted and experimental data.

Keywords

Rotary flexion, Fatigue, ANOVA, Response surface methodology (RSM), Lifetime, Taguchi method.

1. Introduction

Fatigue is defined as the degradation of materials subjected to repeated loading, with potentially damaging consequences. Fatigue failure is one of the most common and critical failure modes in engineering structures. Under cyclic loading, a structural component may exhibit visible cracks or complete fractures after a period of service and repeated loading, even though the stress on the component is less than the static strength of the material. Furthermore, although the material may be elastoplastic, it often fails without undergoing significant plastic deformation. [1]

Operating parameters such as load and hardness play a significant role in the fatigue process and have a direct influence on the life of the mechanism. The negative effect of mean stress on fatigue limit and life is usually modelled using the modified Goodman diagram. However, some experimental results [2-4] have shown that in the case of stainless steels, for the same stress amplitude, the average stress can have a beneficial effect on the number of cycles to failure of the specimen (called fatigue life).

It has been shown that the fatigue life of stainless steels correlates more with the strain range than with the stress amplitude, even in the high cycle range [5]. The design fatigue curve has been established on the basis of the fatigue life obtained in controlled strain fatigue tests [6,7].

Therefore, variations in fatigue life due to mean stress must be compared over the same strain range. The influence of mean stress under controlled stress conditions is critical from a practical point of view. For example, the effect of residual stress is considered in the assessment of thermal fatigue damage [8].

Steels exhibit significant cyclic softening and hardening phenomena under cyclic loading. This makes it complex to study the effect of the average stress for a given strain range, as this varies considerably in controlled loading fatigue tests [9,10].

Thus, ANN has been widely used in various fields of analysis, prediction and classification. It has been presented as an effective tool for analysing the effect of stress ratio on fatigue crack propagation in steel based on experimental test results. Several ANN models have been developed to address different types of fatigue related problems [11-14].

The Taguchi method, developed by Dr Genichi Taguchi in the 1960s [15], is now widely used by many researchers in a variety of studies. It is based on fractional experimental designs, a powerful statistical approach that integrates the design of systems, parameters and tolerances to optimise process and product performance. These designs allow the effects of different factors and their interactions to be taken into account, while significantly reducing the number of trials required [16,17]. The Taguchi method also incorporates concepts such as orthogonal tables, controlled factors, noise factors and signal-to-noise ratio. It is currently widely used in scientific and industrial settings [18-20].

This experimental study focuses on the rotational bending fatigue behaviour of a locally fabricated material. The main objectives are to determine the fatigue limit for a given stress cycle and the endurance limit. The fatigue behaviour of the material has been characterised by tests carried out on a series of identical specimens subjected to specific stress cycles. A statistical analysis of the influence of this operating parameter on the evolution of the number of revolutions (N) was also carried out. The results were statistically analysed using analysis of variance (ANOVA) and response surface methodology (RSM). These results provide a detailed characterisation of the fatigue behaviour of the material, identifying the key parameters and their effects on fatigue life.

2. Experimental tools

2.1 Experimental set-up

The aim of this study is to determine the influence of various fatigue parameters, such as stress and hardness, as well as different surface characteristics, on the service life (evolution of the number of rotations (N)) of hardened C45 steel, expressed in stress cycles until sample failure, using a fatigue testing machine (Fig. 1). For this purpose, sample rods (fig. 2) with different loads, hardnesses and surface roughnesses (detailed in table 1 and the diagram below) were used.

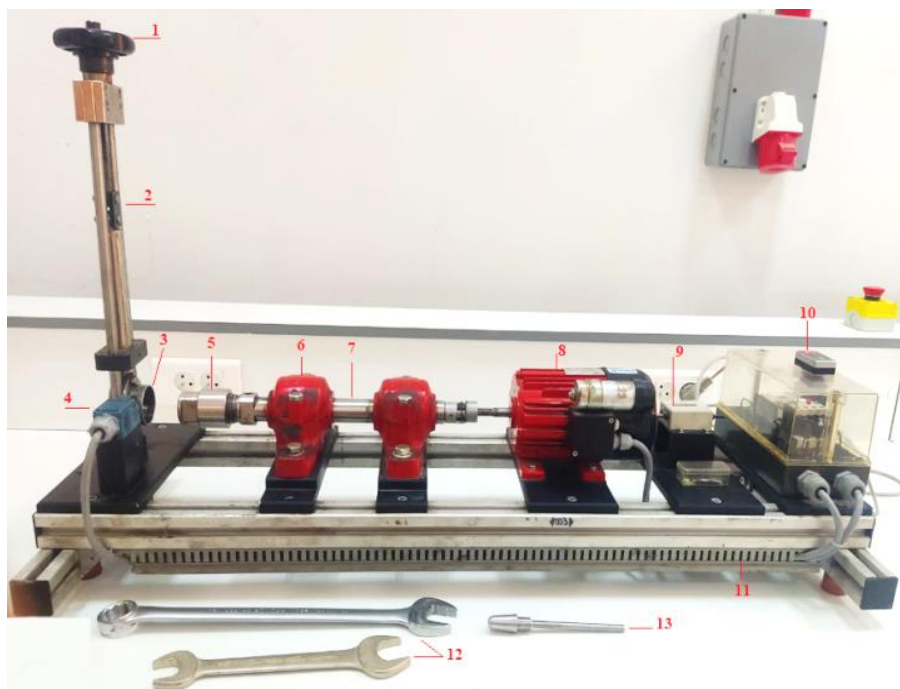


Fig. 1 Experimental set-up (The GUNT WP 140 fatigue testing machine)

1- Handle, 2- Force gage, 3- loading element with ball-bearing, 4- Micro-switch, 5- Chuck, 6- Bearing, 7- Drive shaft, 8- Motor, 9- Counter, 10- Electrical connection with overload switch, 11- Chassis, 12- Spanner, 13- sample rod.

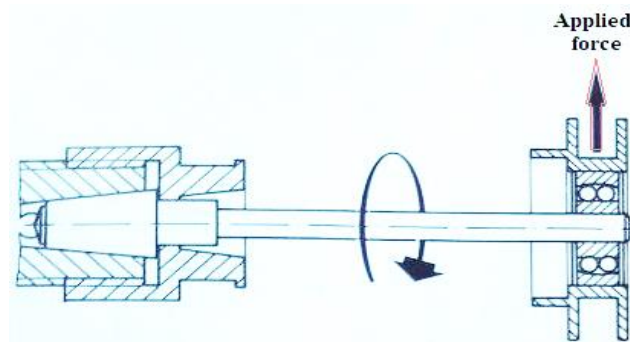


Fig. 2 Applied load on the sample rod

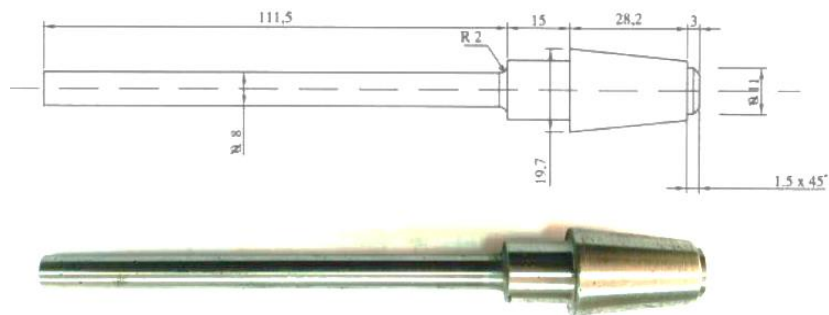


Fig. 3 The sample rod

- Maximum bending stress**

The maximum bending stress σ on the outer fibre is calculated using Navier's formula:

$$\sigma = \frac{M_f}{M_I} \quad (1)$$

With :

M_f : Bending moment relative to the section under consideration ;

M_I : Moment.

$$M_f = F * L \quad (2)$$

F : The load applied.

L : Lever arm length.

and : $M_I = \frac{I}{V} \quad (3)$

I : Moment of inertia of the section in relation to the neutral axis,

$$I = \frac{\pi \cdot d^4}{64} \quad (4)$$

V : Distance from outer fibre to neutral fibre.

$$V = \frac{D}{2} \quad (5)$$

So :

$$M_I = \frac{\pi \cdot d^3}{32} \quad (6)$$

$$\Rightarrow \sigma = \frac{M_f}{M_I} = \frac{32 F * L}{\pi \cdot d^3} \quad (7)$$

$$\sigma \approx 2F \text{ (N/mm}^2\text{)} = \frac{32 F * 100.5}{\pi \cdot 8^3} \quad (8)$$

2.2 Taguchi analysis

The experiments were carried out using the Taguchi method. Hardness (H), surface roughness (Ra) and stress (σ) were chosen as control factors and their values were defined as shown in Table 1.

The L18 (21×32) mixed orthogonal lattice, which is the most appropriate for our study, was used to perform the flexural fatigue tests to determine the life (in number of cycles) of a C45 material, as shown in Table 2.

2.3 Experimental measurements

After setting up the L18 (21×32) mixed orthogonal design using the Taguchi method, the planned tests were carried out. The choice of tables depends mainly on the experimenter, who is responsible for selecting the operating parameters (input variables) and their levels of variation. In our study, we were particularly interested in the response in terms of specimen life, measured by the change in the number of rotations (N). This number of rotations was recorded using a counter and at least three measurements were taken for each sample, with the average being used as the final result.

2.4 Conduct of the study

Input parameters: In this study of the effects of operating parameters, the input factors (problem variables) used in the tests are stress (σ), arithmetic surface roughness (Ra) and hardness (H). Each input factor is varied at three levels, coded as follows: 1, 2 and 3. The levels of variation are given in Table 2 (3 for the upper level. 1 for the lower level. 2 for the base level).

Table 1 The problem variables

Levels	hardness H	surface roughness, Ra (μm)	stress σ (N/mm ²)
1	202	0.075	300
2	247	0.1	360
3	/	0.3	440

Output parameters: The y_i are the output parameters. Sample life (evolution of the number of revolutions (N)): The number of revolutions (N) is measured by a counter. Note that the number of revolutions is measured at least three times up to the endurance limit (the broken specimen) and the average value is taken.

In addition to establishing the relationships between the responses (output parameters) and the input variables (Eq. 9), we are also interested in the strength of the correlation between these parameters and the analysis of the experimental results. In this study we have chosen a quadratic model [21, 22]:

$$Y = f(Q, V, C) + \epsilon \quad (9)$$

Where f is the response function.

ϵ is the model error

$$Y = a_0 + \sum_{i=1}^k a_i \cdot X_i + \sum_{i=1}^k \sum_{i < j}^k a_{ij} \cdot X_i X_j + \sum_{i=1}^k a_{ii} \cdot X_i^2 \quad (10)$$

Where: The term a_0 represents the constant in the model equations, while the coefficients a_1, a_2, \dots, a_k correspond to the linear terms. The coefficients $a_{12}, a_{13}, \dots, a_{ik}$ and $a_{11}, a_{22}, \dots, a_{kk}$ represent the interaction and quadratic terms respectively. X_i denotes the input parameters (H, Ra, and σ).

The experimental results of the specimen life (the evolution of the number of rotations (N)) for different combinations between the input parameters (H, Ra and σ) with the Taguchi L18 experimental design are presented in Table. 2.

Table 2. L18 orthogonal array experimental results for specimen life (the evolution of the number of rotations (N))

N° Tests	Coded factors			Designing parameters			Responses factors N (rpm)	
	X_1	X_2	X_3	H	Ra (μm)	σ (N/mm ²)	Exp	RSM
1	1	1	1	202	0.075	300	18400	22656.8
2	1	1	2	202	0.075	360	8892	13601.0
3	1	1	3	202	0.075	440	2000	5594.5
4	1	2	1	202	0.1	300	16224	11769.8
5	1	2	2	202	0.1	360	7240	11769.8
6	1	2	3	202	0.1	440	1814	-3923.0
7	1	3	1	202	0.3	300	8000	7853.9
8	1	3	2	202	0.3	360	4249	4080.3
9	1	3	3	202	0.3	440	1232	3116.9
10	2	1	1	247	0.075	300	68686	62818.2
11	2	1	2	247	0.075	360	48623	39019.6
12	2	1	3	247	0.075	440	8445	11356.0
13	2	2	1	247	0.1	300	47503	51495.6
14	2	2	2	247	0.1	360	14859	28283.8
15	2	2	3	247	0.1	440	4690	1402.8
16	2	3	1	247	0.3	300	41875	44093.8
17	2	3	2	247	0.3	360	30000	25577.4
18	2	3	3	247	0.3	440	4323	4956.8

3. Results and discussion

3.1 Statistical analysis of results

The experimental data were processed by quadratic regression using Minitab16 software, which allowed us to determine the influence of the operating parameters on the life of the specimen, expressed as the evolution of the number of rotations (N).

3.1.1 Analysis of Variance of Lifetime (Number of rotations) (ANOVA)

The main results of the analysis of variance (ANOVA) for the evolution of the number of rotations (N) of the specimen are presented in Table 3.

Table 3. ANOVA results for specimen life (N)

Source	DF	SS	MS	F-value	P-value	Pc (%)	Remarks
Regression	8	6345410294	793176287	14.5072	0.000268	/	significant
H	1	2243450456	1346121478	24.6205	0.000778	32.81*	
Ra	1	171951727	249561975	4.5645	0.061373	2.51	
σ	1	2634290160	59995108	1.0973	0.322173	38.53*	
H.Ra	1	13859719	13859719	0.2535	0.626717	0.20	
H. σ	1	893553573	893553573	16.3431	0.002917	13.07*	
Ra. σ	1	91893518	91893518	1.6807	0.227081	1.34	
Ra.Ra	1	284335447	284335447	5.2005	0.048526	4.16	
σ. σ	1	12075693	12075693	0.2209	0.649561	0.18	
Error	9	492072759	54674751			7.20	
Total	17	6837483054					

DF: degree of freedom; **SS:** sum of squared deviations; **MS:** mean square; **F-value:** variance test; **P-value:** probability; **Pc:** percentage contribution (%). The model coefficients for the corresponding response are estimated using the regression analysis technique for a significance level of $\alpha = 5\%$ ($P\text{-value} < \alpha$ the source factor is significant) and a confidence level of 95%. [20]

In the ANOVA (Table 3) it is clearly observed that the applied stress (with a contribution of 38.53%) is the main factor influencing the evolution of the number of rotations (N). It is followed by hardness (H) with a contribution of 32.81%, while the interaction between hardness and applied stress (H.σ) also has a significant effect on fatigue life with a contribution of 13.07%. On the other hand, the other parameters have a much smaller effect with contributions such as Ra: 2.51%, H.Ra: 0.20% and Ra.σ: 1.34%.

Furthermore, the analysis of these results (Table 3) allowed us to develop the following mathematical model:

$$N = -354552 + 2559.62 H - 798099 Ra + 682.987 \sigma - 387.314 H*Ra - 5.46031 H*\sigma + 1.84843 \times 10^6 Ra*Ra + 391.279 Ra*\sigma + 0.363209 \sigma*\sigma \quad (11)$$

($R^2=92.80\%$, $\text{Adjusted } R^2=86.41\%$)

Table 3 shows the results of the quadratic ANOVA model. The quality of the model established (equation 11) for the life of the specimen, measured by the evolution of the number of rotations (N), is evaluated by the correlation coefficients R^2 and R^2 adjusted, which are 92.80% and 86.41% respectively. These values indicate that the responses are very well explained by the proposed regression model.

Figure 4 shows the effect of the main factors on the average values of specimen life (measured by the evolution of the number of rotations, N). It is clear that the life is a decreasing function of stress (σ) and roughness (Ra). On the other hand, it also appears that life N is an increasing function of hardness (H).

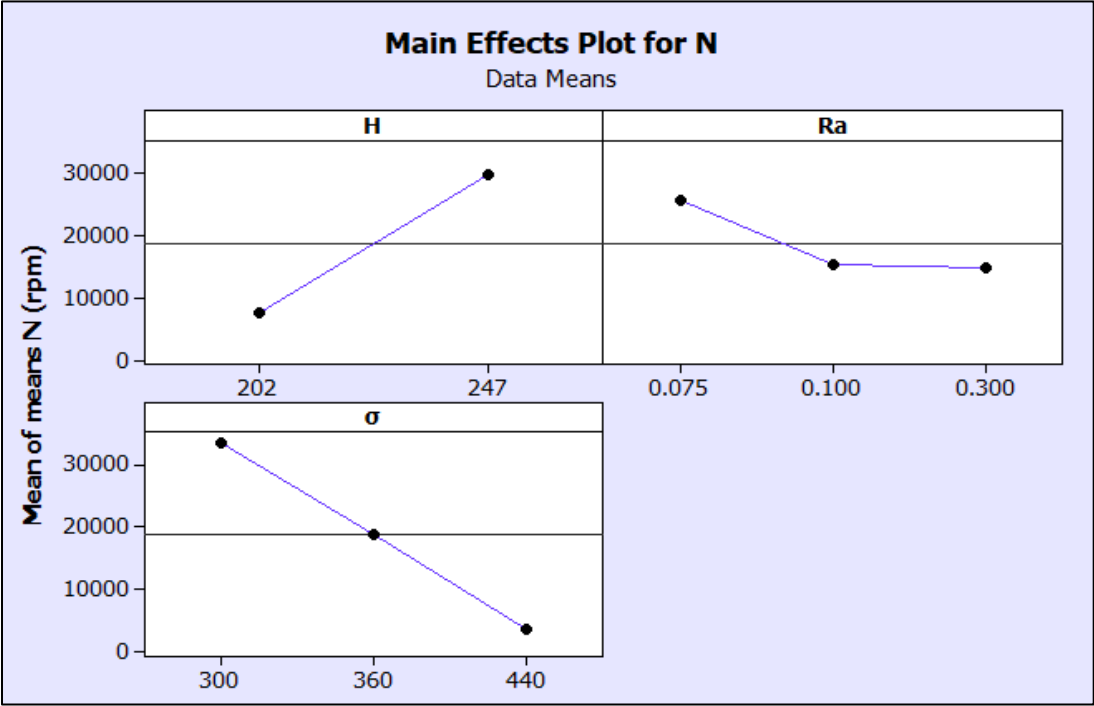


Fig. 4. Main factor effects on lifetime (the evolution of rotation number N).

To better visualize the effects of the operating parameters (H, Ra, and σ) on the evolution of the number of rotations (lifetime N), 3D plots and contour curves are shown in Figures 5 and 6. These figures, generated using Response Surface Methodology (RSM), help identify the optimal operating conditions.

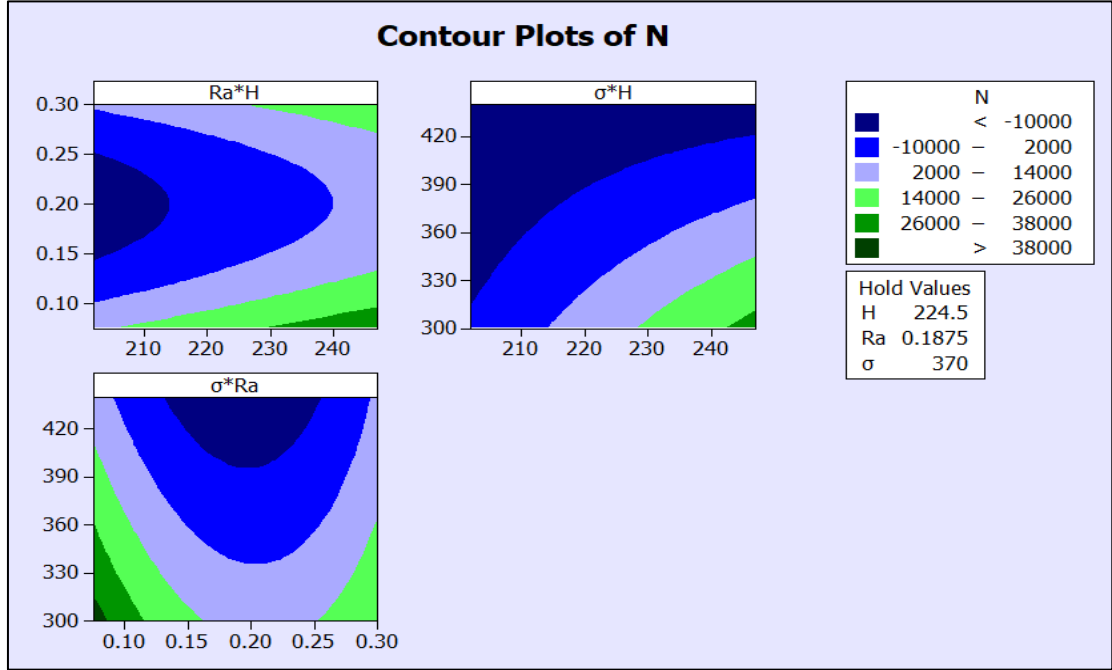


Fig. 5 Contour Plots of lifetime N

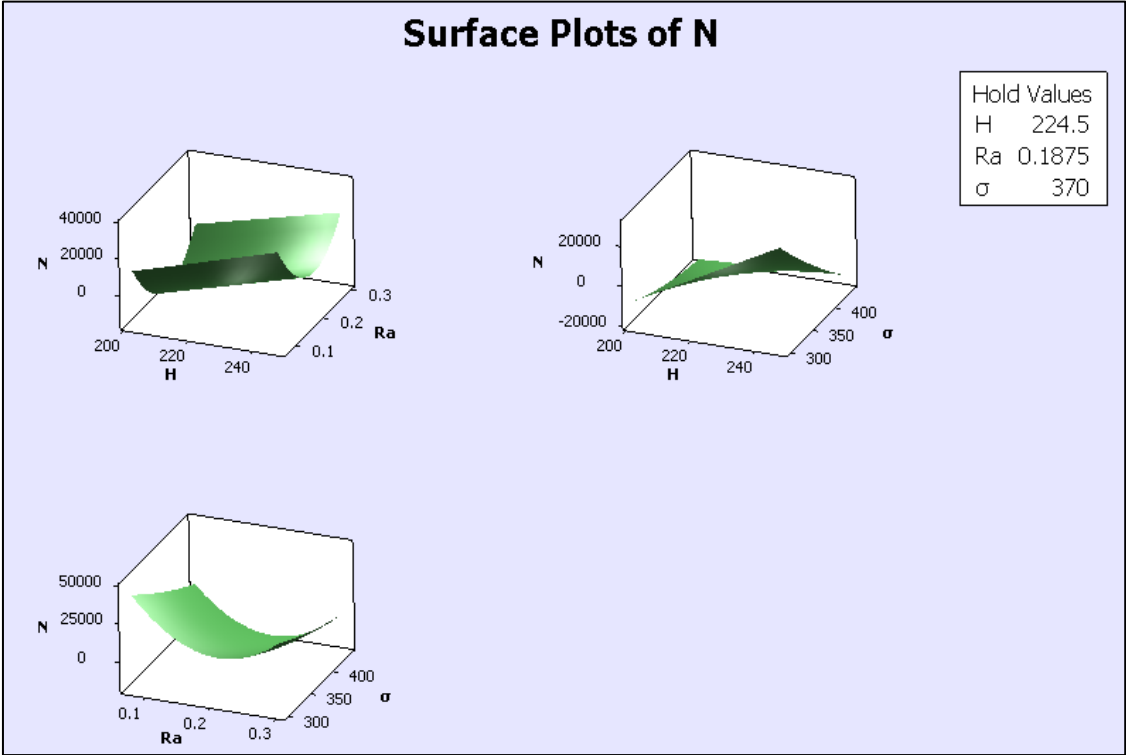


Fig. 6. 3D Surface Plots of lifetime N

From the results shown in Figures 5 and 6, it is clear that service life increases with increasing material hardness and decreases with decreasing material hardness. It is also clear from these figures that the highest life (in terms of number of revolutions) is achieved when operating at low levels of applied stress and surface roughness.

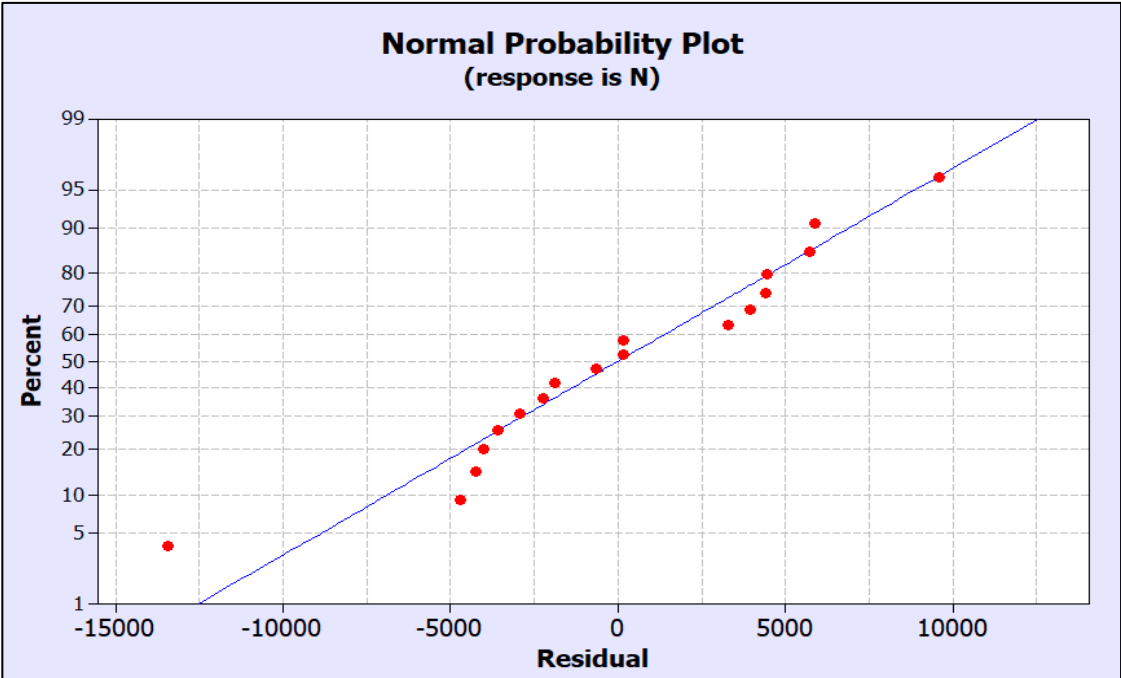


Fig 7 Normal probability plot of the residuals for lifetime N

Furthermore, Figure 7, which shows the normal probabilities of the residuals of the RSM model (with respect to life N), clearly shows that the residuals are almost perfectly fitted to the straight line. This indicates that the errors follow a normal distribution, confirming that the terms of the fitted model are significant.

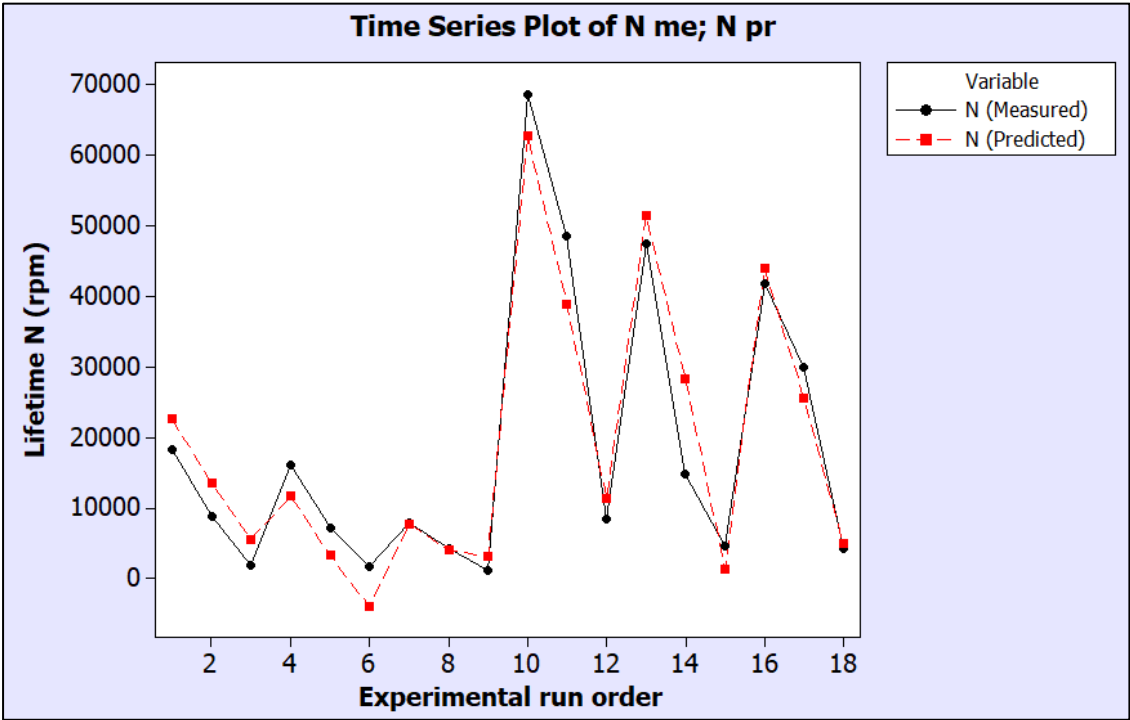


Fig 8 Measured and predicted values of Lifetime N

From Figure 8, the results show excellent agreement between the experimental data and the predictions, indicating that the developed model is both consistent and better suited to estimating specimen life.

3.2 Photographs and photomicrographs of the specimens after the operation

In order to better understand the phenomenon of fatigue as a function of operating parameters (hardness, roughness, stress), photomicrographs are taken using a light microscope (Euromex type).

Figure 9 characterises the appearance of the test piece before the operation and figure 10 gives a detailed image of the test pieces after the operation.



Fig 9 Photographs of the specimens before operation.



Fig 10 Photographs of the specimens after operation.

The fracture surface of the specimen shows numerous radial lines distributed over the entire circumference (Figure 11), indicating that the fatigue process leading to fracture initiated at multiple points on the specimen surface.

This indicates that the highest stress concentrations were at the fillet, although their small extent suggests moderate loading of the part. Examination of the initiation zone also reveals the presence of numerous micro-cracks on the surface of the fillet.

In Figure 12, it can be seen that the fracture zone of heat-treated samples is smaller than that of untreated samples (Figure 11). This suggests that heat treatment helps to increase the life of the samples.

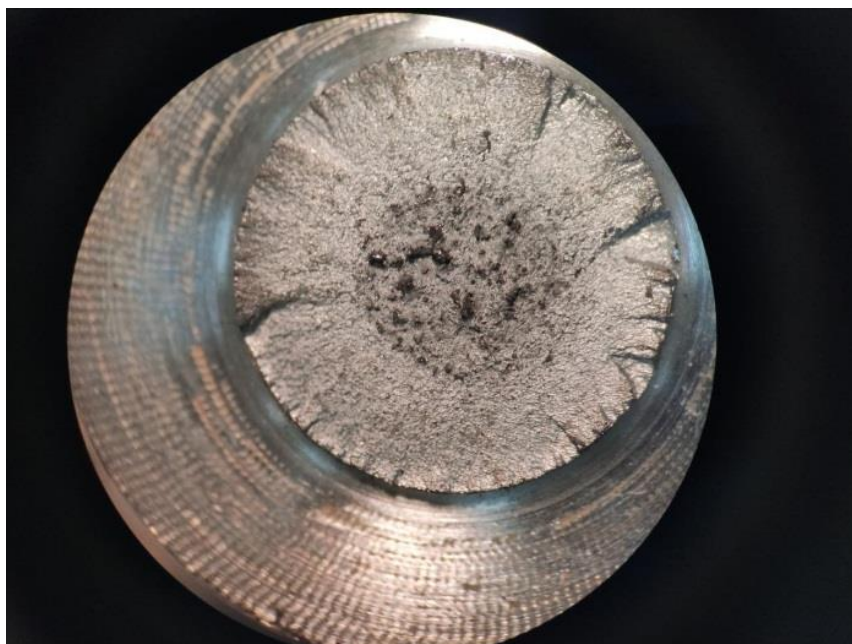


Fig. 11 Optical photomicrograph (magnification, x20) of the fracture surface of a rotating bending fatigue test specimen under a stress of 300 N/mm^2 and $Ra=0.075\mu\text{m}$ after 18400 cycles (crude steel $H_v = 202$).



Fig. 12 Optical photomicrograph (x20 magnification) of the fracture surface of a rotary bending fatigue test specimen at a stress of 360 N/mm^2 and $Ra = 0.075$ after 48623 cycles of C 45 steel quenched at 850°C and tempered at 200°C ($H_v=247$).

4 Conclusions

In this study, the Taguchi method and Response Surface Methodology (RSM) were used to evaluate the effect of operating parameters and material properties on specimen life (in number of rotations). The analysis aimed to establish the relationship between operating conditions such as hardness (H), surface roughness (Ra) and stress (Q) and the responses of interest, in particular specimen life (N).

The main conclusions that can be drawn from this study are:

- The life of the specimen (the evolution of the number of revolutions (N)) decreases in proportion to the load applied and the arithmetic roughness, and is inversely proportional to the hardness.
- Steel quenched at 850°C and tempered at 200°C has a higher fatigue limit than unalloyed steel, so heat treatment increases the life of the specimens.
- The size of the fracture zone is smaller for specimens that have been heat treated than for those that have not.
- The condition of the surface (roughness) and the environment are parameters that can significantly affect the life of a material.
- The analysis of variance (ANOVA) showed that the applied stress (contribution: 38.53%) is the main factor with the greatest influence on the evolution of the number of revolutions (N), followed by the hardness factor (H) with 32.81%, followed by the interaction between hardness and applied stress ($H.\sigma$) with a contribution of 13.07%. On the other hand, the effects of the other parameters were found to be very small.
- The coefficient of determination R^2 for the lifetime determined by ANOVA is satisfactory, demonstrating the suitability of the proposed model.

Nomenclature

Mf: Bending moment relative to the section under consideration.

MI: Moment.

F: The load applied.

L: Lever arm length.

I: Moment of inertia of the section in relation to the neutral axis,

V: Distance from outer fibre to neutral fibre.

H: Hardness

σ : stress

Ra: Arithmetic surface roughness

N: Sample life (evolution of the number of revolutions)

y_i are the output parameters

f: the response function.

ϵ : the model error

X_i : denotes the input parameters

a_1, a_2, \dots, a_k : The linear terms

$a_{12}, a_{13}, \dots, a_{ik}$: The interacting terms

$a_{11}, a_{22}, \dots, a_{kk}$: The quadratic terms

DF: degree of freedom;

SS: sum of squared deviations;

MS: mean square;

F-value: variance test;

P-value: probability;

Pc: percentage contribution (%)

REFERENCES

- [1] Yusong Pan a, Pan Wu a, Shuaiqi Fan b, Xulong Peng c, Ziguang Chen Peridynamic, Simulation of fatigue crack growth in porous materials, *Engineering Fracture Mechanics*, 300 (2024) 109984. <https://doi.org/10.1016/j.engfracmech.2024.109984>
- [2] J. Colin, A. Fatemi, S. Taheri, Fatigue behavior of stainless steel 304L including strain hardening, prestraining, and mean stress effects, *Journal of Engineering Materials and Technology*. 132 (2010) no.021008, 1-13. <https://doi.org/10.1115/1.4000224>
- [3] Masayuki Kamaya, Masahiro Kawakubo, Mean stress effect on fatigue strength of stainless steel, *International Journal of Fatigue*, 74 (2015) 20-29. <https://doi.org/10.1016/j.ijfatigue.2014.12.006>
- [4] N. Miura, Y. Takahashi, High-cycle fatigue behavior of type 316 stainless steel at 288 °C including mean stress effect, *International Journal of Fatigue*. 28 (2006) 1618-1625. <https://doi.org/10.1016/j.ijfatigue.2005.07.051>
- [5] Julie Colin, Ali Fatemi, Said Taheri, Cyclic hardening and fatigue behavior of stainless steel 304L, *Journal of Materials Science*, 46 (2011) 145-154. <https://link.springer.com/article/10.1007/s10853-010-4881-x>
- [6] Omesh K. Chopra, William J. Shack, Low-cycle fatigue of piping and pressure vessel steels in LWR environments, *Nuclear Engineering and Design*, 184 (1998) 49-76. [https://doi.org/10.1016/S0029-5493\(97\)00368-3](https://doi.org/10.1016/S0029-5493(97)00368-3)
- [7] Noelia Olivia Fuentes Solis, Serguei Gavrilov, Erich Stergar, Marc Seefeldt, Martine Wevers, Pierre Marmy, Statistical analysis of the effect of lead-bismuth eutectic on fatigue resistance of 316L, *Nuclear Engineering and Design*, 407 (2023) 112312. <https://doi.org/10.1016/j.nucengdes.2023.112312>
- [8] F. Szmytka, E. Charkaluk, A. Constantinescu, P. Osmond, Probabilistic Low Cycle Fatigue criterion for nodular cast-irons, *International Journal of Fatigue*, 139 (2020) 105701. <https://doi.org/10.1016/j.ijfatigue.2020.105701>
- [9] Ludovic Vincent, Jean-Christophe Le Roux, Said Taheri, On the high cycle fatigue behavior of a type 304L stainless steel at room temperature, *International Journal of Fatigue*, 38 (2012) 84-91. <https://doi.org/10.1016/j.ijfatigue.2011.11.010>
- [10] M.S. Cagle, K.E. Bryan, M. Dantin, W.M. Furr, D. Giri, B. Huddleston, A. Hudson, S. Mujahid, K. Tantratian, A.K. Persons, F. Smith, R. Stokes, M. F. Horstemeyer, Characterization and modeling of the fatigue behavior of 304L stainless steel using the MultiStage Fatigue (MSF) Model, *International Journal of Fatigue*, 151 (2021) 106319. <https://doi.org/10.1016/j.ijfatigue.2021.106319>
- [11] S. Ramachandra, J.F. Durodola, N.A. Fellows, S. Gerguri, A. Thite, Experimental validation of an ANN model for random loading fatigue analysis, *International Journal of Fatigue*, 126 (2019) 112-121. <https://doi.org/10.1016/j.ijfatigue.2019.04.028>
- [12] P. Artymiak, L. Bukowski, J. Feliks, S. Narberhaus, H. Zenner, Determination of S-N curves with the application of artificial neural networks, *Fatigue & Fracture of Engineering Materials & Structures*, 22 (1999) 723-728. <https://doi.org/10.1046/j.1460-2695.1999.t01-1-00198.x>
- [13] F. Iacoviello, D. Iacoviello, M. Cavallini, Analysis of stress ratio effects on fatigue propagation in a sintered duplex steel by experimentation and artificial neural network approaches, *International Journal of Fatigue*, 26 (2004) 819-828. <https://doi.org/10.1016/j.ijfatigue.2004.01.004>
- [14] Karthik Reddy Lyathakula, Fuh-Gwo Yuan, A probabilistic fatigue life prediction for adhesively bonded joints via ANNs-based hybrid model, *International Journal of Fatigue*, 151 (2021) 106352. <https://doi.org/10.1016/j.ijfatigue.2021.106352>
- [15] J. Antony. Taguchi or Classical design of experiments: a perspective from a practitioner. *Sensor Review*, 26 (2006) 227-230. <https://doi.org/10.1108/02602280610675519>
- [16] Ranjit K. Roy, A Primer on the taguchi method, Society of Manufacturing Engineers, Second edition, 2010.
- [17] Glen Stuart Peace, Taguchi Methods: A Hands-on Approach, Addison-Wesley, 1993.
- [18] G. Venkateswarlu, M. J. Davidson and G. R. N. Tagore, Influence of process parameters on the cup drawing of aluminium 7075 sheet, *International Journal of Engineering, Science and Technology*, 2 (2010) 41-49. <https://www.ajol.info/index.php/ijest/article/view/64553>.
- [19] Raynard Christianson Sanito, Marcelo Bernuy-Zumaeta, Wei-Chien Wang, His Hsien Yang, Sheng-Jie You, Ya-Fen Wang, Optimization of metals degradation and vitrification from fly ash using Taguchi design combined with plasma pyrolysis and recycling in cement construction, *Journal of Cleaner Production*, 387 (2023) 135930. <https://doi.org/10.1016/j.jclepro.2023.135930>
- [20] Fatima Zohra Derdour, Mohamed Kezzar, Lakhdar Khochmane, Optimization of penetration rate in rotary percussive drilling using two techniques: Taguchi analysis and response surface methodology (RMS), *Powder Technology*, 339 (2018) 846-853. <https://doi.org/10.1016/j.powtec.2018.08.030>
- [21] Kanak Kalita, Partha Dey, Milan Joshi and Salil Haldar, Response surface modelling approach for multi-objective optimization of composite plates. *Steel and Composite Structures*, 32 (2019) 455-466. <https://doi.org/10.12989/scs.2019.32.4.455>
- [22] Kanak Kalita, Partha Dey, Salil Haldar. Search for accurate RSM metamodells for structural engineering. *Journal of Reinforced Plastics and Composites*, 38 (2019) 995-1013. <https://doi.org/10.1177/0731684419862346>